

## ULTRASONOGRAPHIC, COMPUTED TOMOGRAPHIC, CT- ARTHROGRAPHIC DESCRIPTION OF NORMAL INTRA- ARTICULAR ANATOMY OF THE CANINE STIFLE: A CADAVERIC COMPARATIVE STUDY

Giulia MORETTI<sup>1</sup>, Mario MILITI<sup>1</sup>, Alexandra PETEOACA<sup>2</sup>, Giovanni ANGELI<sup>1</sup>,  
Eleonora MONTI<sup>1</sup>, Antonello BUFALARI<sup>1</sup>

<sup>1</sup>University of Perugia, University Department of Veterinary Medicine, 4 Via S. Costanzo,  
Perugia, Italy

<sup>2</sup>University of Agronomic Sciences and Veterinary Medicine of Bucharest, 59 Marasti Blvd,  
District 1, Bucharest, Romania

Corresponding author email: giuliamoretti89@gmail.com

### Abstract

*Cranial cruciate ligament (CCL) rupture is a common orthopedic disease in canine patients. Although it is possible to diagnose this injury through an orthopedic clinical examination, imaging can increase diagnostic certainty. This comparative Ex-Vivo study allowed us to improve our knowledge of the ultrasound anatomy of intra-articular structures of the dog's healthy knee. The CCL, the patellar tendon and menisci were examined by ultrasonography, Computed Tomography (CT) and CT-arthrography. Besides performing a comparison of the ultrasound and CT results, to better understand the sonoanatomy of the CCL and to prove that it can be properly identified by sonography, the ligament was stained with methylene blue under ultrasound guidance. To overcome the limitations of the Ex-Vivo study, the ultrasound scans obtained were compared with similar ones performed in healthy non-sedated dogs. Results indicate that in large dogs, ultrasonography is a valid diagnostic method for visualizing the cranial-distal part of the CCL and also evaluating the external portion of both menisci.*

**Key words:** cranial cruciate ligament, dog, ultrasonography, computed tomography.

### INTRODUCTION

Rupture of the Cranial Cruciate Ligament (CrCL) is one of the main cause of lameness in dogs, also representing the major cause of knee osteoarthritis in this species. (Elkins et al., 1991; Johnson et al., 1994; Witsberger et al., 2008). The aetiology of the rupture of the CrCL is complex and multifactorial, concerning traumatic, degenerative, conformational, anatomical and autoimmune factors (Cook, 2010; Griffon, 2010; Sanchez-Bustinduy et al., 2010). Rupture of the Cranial Cruciate Ligament is a commonly diagnosed as a bilateral event (De Bruin et al., 2007; Cabrera et al., 2008; Buote et al., 2009; Grierson et al., 2011; Fuller et al., 2014). Most of injury occurs in the absence of a triggering traumatic event, in these cases, the lesion is the result of a chronic ligamentous degeneration (Gambardella et al., 1981; Galloway et al., 1995). The ligament gradually undergoes degenerative phenomena that they can lead to its partial rupture or, more

belatedly, to a complete one (Duval et al., 1999; Griffon, 2010). Furthermore, in association with the rupture of CrCL, it is common to observe lesions affecting the medial meniscus, in particular its caudal portion (Rey et al., 2014; Ritzo et al., 2014). However, in case of partial ligament lesions or meniscal lesions in the early stage, the only clinical examination does not allow to achieve a clear diagnosis. Therefore, diagnostic imaging techniques have recently acquired an essential role in confirming the diagnosis, issuing the prognosis and planning the surgery of orthopedic diseases. In Veterinary Medicine, radiography was the first diagnostic technique for imaging used in case of suspected rupture of the CrCL. However, the X-ray exam does not allow to directly view the injured CrCL but only shows the osteoarticular degenerative lesions ensuing its rupture (Marino et al., 2010). Magnetic Resonance is the elective instrumental investigation for the study of joint pathologies, but it is an expensive tool and not so available

to be part of the common veterinary clinical practice. (Banfield & Morrison, 2000; Ohlert et al., 2001; Vande Berg et al., 2002; Soler et al., 2007; Scrivani, 2018).

Arthroscopy, which is characterized by high diagnostic sensitivity, is a common technique used for the diagnosis and treatment of rupture of the CrCL and meniscal tears, although, compared to the previously mentioned methods, it shows a certain degree of invasiveness. (Thieman et al., 2006; Pozzi et al., 2008; Plesman et al., 2013; Ritzo et al., 2014). For the reasons mentioned above, in the last few years, the attention has turned to two diagnostic techniques less used previously: Ultrasound and Computed Tomography (CT). The CT exam is an increasingly used diagnostic method in the diagnosis of knee pathologies, denoting a high sensitivity in the diagnose hard tissue diseases. On the other hand, the real usefulness of the CT examination in the study of teno-ligamentous structures is controversial (Samii& Dyce, 2004; Han et al., 2008). Knee ultrasound is a method studied since the second half of the 90s which, with the development of technologies increasingly innovative, has made significant progress in the identification and study of the main intra-articular structures. In our view, given the recent development of high-frequency ultrasound probes more advanced than those used in the past is required a new sono-anatomical evaluation of the main intra-articular structures of the healthy knee of the dog aimed to identify the limits and strengths of this diagnostic method.

The main purpose of this Ex-Vivo study was to broaden the knowledge over the ultrasound anatomy of the main intra-articular structures of the healthy knee of the dog, assessing the strengths and weaknesses of the diagnostic method. In addition, in order to understand the sono-anatomy of the CrCL, a comparison was made between ultrasound images and CT scans also with the benefit of CT-Arthrography (CTA).

## MATERIALS AND METHODS

All dogs included in the Ex-Vivo study died from causes unrelated to pathologies affecting the knee joint at the Veterinary Teaching Hospital (OVUD) of the Department of

Veterinary Medicine of Perugia. The presence of bone pathologies was excluded by CT examination, while the integrity of the teno-ligamentous and meniscal structures was verified by performing an arthrotomy.

A total of 14 knees from 8 dogs were examined, all of them weighed more than 25 kg. Whenever possible the corpses were evaluated through ultrasound, CT and CTA without disarticulating the limbs from the rest of the carcass. In some case only the hind limb was isolated disarticulating it at the level of the coxo-femoral joint. The corpses were stored in a cold room for a maximum of 72 hours.

### Ultrasound examination

All the knees subjected to ultrasound examination undergone to trichotomy; abundant isopropyl alcohol and ultrasound gel was used as well. The corpses or individual hind limbs were placed for all ultrasound scans in lateral recumbency with the joint to be examined uppermost. A Voluson® P6 GE scanner was used. For the evaluation of the patellar tendon, the infrapatellar fat pad, the CrCL and Menisci, the linear high frequency (5-15 MHz) probe was used, while for caudal scans of the knee we opted both for a convex (2-5 MHz) or a linear high frequency (5-15 MHz). The stifle joint was investigated ultrasonographically in the sagittal and transverse planes. The acoustic windows used were obtained by cranial, medial, lateral and caudal approach. The patellar tendon, the fat pad infrapatellar and the profile of the femoral condyles were assessed by scanning the cranial window with the linear probe positioned longitudinally. In the same scan, bringing the knee to its maximum flexion, allowed the Cranial Cruciate Ligament to be seen/identified (Figure 1).



Figure 1. Cranial longitudinal ultrasonographic scan of the Cranial cruciate ligament (asterisk) and Patellar tendon (white arrow)

Sometimes, rotating the probe 20° in the proximolateral-dystomedial direction it was possible to obtain more detailed images of the cranial portion of the CrCL. The medial meniscus was visualized longitudinally from the medial knee compartment in semi-flexion; scanning the lateral compartment the lateral meniscus could be assessed. Moving the probe slightly in the cranio-caudal direction it was also possible to evaluate the medial and lateral collateral ligaments. Through the investigation of the cranio-lateral area of the knee joint, the tendon of the extensor digitorum longus muscle can be identified cranially to the lateral collateral ligament (Table 1). Caudal scans were performed both via a convex probe and via a high-frequency linear probe. The probe was placed on the joint compartment caudal and was oriented transversely or longitudinally.

Table 1. Evaluation criteria used for ultrasound to evaluate the menisci, patellar tendon and cranial cruciate ligament

Structure	Criteria	Ultrasound
Cranial cruciate ligament	Overall visibility	0: Not visible
		1: Visible
	Visibility of the contour	0: Not visible
		1: Barely visible
2: Moderately visible		
Linearity of the contour	0: Irregular outline	
	1: Regular outline	
Appearance of the internal structure	0: No longitudinal echoes detected	
	1: Moderate longitudinal pattern	
	2: Clear longitudinal pattern	
Menisci	Overall visibility of the external portion of the meniscal body	0: Not visible
		1: Barely visible
		2: Moderately visible
		3: Clearly visible
	Appearance of the internal structure	0: Non Homogeneous
		1: Homogeneous
Shape	0: Not triangular	
	1: Partially triangular	
		2: Clearly triangular

### CT examination

For the CT and CTA exam, all data was collected using the TC scanner HD 16 sections (Fujifilm-FCT-Speedia). The carcasses were positioned in sternal recumbency, while the individual hind limbs were placed with the cranial compartment of the knee in contact with the table. The flexion angle of the knees ranged from 110° to 130°.

To obtain the images the parameters were set at 140 kilovolts (kV) and 170 milliamperere (mA). The layer thickness was 0.65 mm.

The acquired images were evaluated with a medical imaging DICOM viewer (Horos™).

CT images were evaluated by applying an algorithm for both hard and soft tissue (Table 2). The CTA scans were studied using a single algorithm. The appearance and length of the CrCL were evaluated in a multiplanar reconstruction on a parasagittal plane. The width was measured in its distal third (Table 3). The lateral meniscus-femoral ligament was studied on the frontal plane. The menisci were evaluated axially. Arthrocentesis was performed using a 23-gauge needle inserted into the lateral parapatellar recess. The iodinated contrast was initially inoculated in all dogs at a volume of 3 ml (Iobitridol, Xenetix, Guerbet spa, Italy) with a concentration of 150 mg/ml.

Table 2. Evaluation criteria used for Computed Tomography (CT) to evaluate the cranial and caudal cruciate ligament, menisci and lateral menisco-femoral ligament

Structure	Criteria	CT
Cranial cruciate ligament	Overall visibility	0: Not visible
		1: Barely visible
		2: Moderately visible
Caudal cruciate ligament	Visibility of the contour	3: Clearly visible
		0: Not visible
		1: Barely visible
Lateral menisco-femoral ligament	Appearance of the internal structure	2: Moderately visible
		3: Clearly visible
		0: Non Homogeneous
Menisci		1: Homogeneous

Table 3. Evaluation criteria used for Computed Tomography Arthrography (CTA) to evaluate the cranial and caudal cruciate ligament, menisci and lateral menisco-femoral ligament

Structure	Criteria	CTA
Cranial cruciate ligament	Overall visibility	0: Not visible
		1: Barely visible
		2: Moderately visible
Caudal cruciate ligament	Distribution of the contrast medium	3: Clearly visible
		0: Low
Lateral menisco-femoral ligament	Appearance of the internal structure	1: Moderate
		2: Good
Menisci		0: Non Homogeneous
		1: Homogeneous

### Inoculation of methylene blue and arthrotomy

In all the knees examined by ultrasound, after performing the CTA, a 22 G spinal needle was inserted echo-guided inside the joint cavity. After penetrating the CrCL, a minimal amount of methylene blue (0.05 ml) was placed in the ligament. An arthrotomy was subsequently performed to evaluate the CrCL and the quality of staining.

### ***In vivo* study**

In the comparative *in vivo* study were included 6 healthy dogs weighing more than 25 kg. No animal was sedated or anesthetized. Given the intent to exclude the presence of related pathologies of the knee, the animals were subjected to an orthopedic examination: in each patient a thorough anamnestic investigation was conducted, followed by inspection examination (gait and posture analysis) and specific orthopedic examination of the joint (external palpation, flexion-extension - specific tests for the exclusion of lesions affecting the CrCL). The same devices and scans applied for cadavers were used to evaluate the knees in these dogs. In addition, all the images were evaluated with the same criteria.

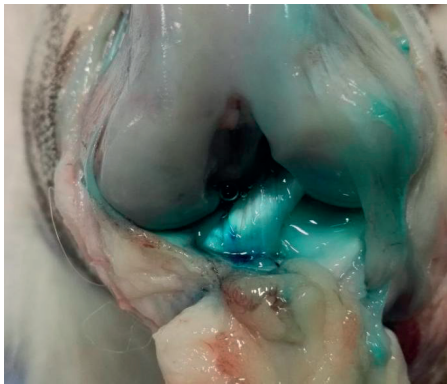


Figure 2. Arthrotomic visualization of the cranial cruciate ligament stained by methylene blue through ultrasonographic guide

## **RESULTS AND DISCUSSIONS**

14 knees from 8 corpses were included in the cadaveric study. The corpses belonged to different breeds: Great Dane, Boxer, Czechoslovakian Wolfdog, Golden Retriever, Swiss Shepherd, German Shepherd, Hound, Mixed breed. Moreover, a total of 12 knees from 6 healthy dogs were included in the *In-Vivo* study. The examined subjects belonged to the following breeds: Dobermann, Labrador Retriever, American Pit Bull Terrier, Weimaraner. In this study, there were also two large mixed breeds. All subjects included in our study weighed more than 25 kg. Whenever possible, the corpses were evaluated by ultrasonography, CT and CTA without disarticulating the limbs from the rest of the

carcass: the aim was to simulate the normal positioning of the animal during these examinations. We performed the US-scans with a high frequency linear probe (5-15 MHz), which has a uniform insonation angle limiting the artifacts due to anisotropy. The hypoechoic aspect of CrCL described in previous studies (Kramer et al., 1999; Soler et al., 2007) is probably associated to these artifacts.

Through ultrasonography the CrCL was visible in all cases both *ex vivo* and *in vivo* (14/14 *ex vivo*, 12/12 *in vivo*) (Table 4). This structure was seen, in all cases, as a clearly hyperechoic portion in the part closest to the tibial insertion, continued by a proximal low echogenicity portion. The CrCL showed in most cases a clearly visible and linear contour, both *ex vivo* (clearly visible 57.14%, linear 78.57%) and *in vivo* (clearly visible 58.33%, linear 78.57%). In 64.28% of cases *ex vivo* and 75% *in vivo* the hyperechoic portion showed a clear fibrillar pattern similar to the patellar tendon. *Ex vivo*, the CrCL hyperechoic distal portion showed a length ranging from 28.47% to 58.29% (average of 36.17%) of the total extension of the CrCL obtained in CTA. Moreover, the hyperechoic fibrillar portion showed a length ranging from 56.66% to 97.38% (mean of 74.17%) of the total extent of the ligament that can be ultrasound appreciated. The ultrasound visible total ligament measure ranges from 34.48% to 63.48% (average of 48.95%) of the total length visible in CTA. The estimates relating to the ultrasound visibility of the CrCL agrees with what was described by Van der Vekens et al. (2019). According to our knowledge, no scientific report has ever evaluated the *ex vivo* width of the CrCL appreciable by ultrasound. Taking as a reference the rough point linearity and width of the echoes, which is on average 5.87 mm (median 5.51 mm) from the distal ligament width limit, the maximum ligament width could be measured, which represents 52.57% (from 37.5% to 73.33%) of the total width of the CrCL measured in CTA. The total CrCL width in CTA in all cases was estimated in the distal third, location of the maximum thickness of the CrCL as we found in all the examined scans. In CTA, the average distance between 2/3 of the ligament and the distal point of maximum visibility was equal to 6.85 mm.

Table 4. *Ex vivo* results of the ultrasonographic evaluation of the cranial cruciate ligament (CrCL) and patellar tendon (PT)

Criteria	Ultrasound examination	CrCL	PT
Overall visibility	Not visible	0	
	Visible	14	14
Visibility of the contour	Not visible	0	0
	Barely visible	3	0
	Moderately visible	3	0
	Clearly visible	8	14
Linearity of the contour	Irregular outline	3	
	Regular outline	11	14
Appearance of the internal structure	No longitudinal echoes detected	1	0
	Moderate longitudinal echo-pattern	4	0
	Clear longitudinal echo-pattern	9	14

The maximum CrCL width appreciable on ultrasound is a data which must be critically assessed: despite the measuring point of the ultrasound width (5.87 mm from the distal ligamentous limit) and measuring point of the CTA width (6.85 mm from the distal ligament limit) are very close to each other, it is not clear whether this data is due to a diagnostic limit, or a discrepancy between the two measurement points. Indeed, the CrCL is an anatomically complex structure, which does not have a uniform thickness along its course and its width can vary depending on the knee flexion angle (Heffron & Campbell, 1978). In addition, the measurements in ultrasound knee flexion angle showed different values from the measured in the CT study one. Consequently, it is not easy to assess if the limitation of ultrasonography to estimate only 52.57% of the CrCL width viewed in CTA is due to the inability of the method itself to view the remaining 47.43%, or is attributable to a hypothetical bias in measurements in different points of the ligament. The proximal portion of the CrCL has poor echogenicity and lacks a clear fibrillar pattern, finding in our opinion poor applicability in clinical practice. On the other hand, the distal portion of the CrCL, given its hyperechoic and fibrillar aspect, would make it easier to visualize any ligament injuries present there. To prove the ultrasound visibility of the CrCL a spinal needle was ultrasonographically introduced into the joint cavity of cadavers, inoculating blue of methylene between the fibers of the ligament. As demonstrated by the execution of arthrotomy, in all anatomical preparations in which this maneuver was performed, the CrCL was correctly identified and stained, unequivocally demonstrating the

ultrasound visibility of the ligament. The portion of CrCL dyed has always been the distal one, further confirming the results obtained in the ultrasound and CTA evaluation of the CrCL.

In Ultrasound examination the medial (MM) and the lateral meniscus (LM) were identified in all cases in both the *ex vivo* and *in vivo* evaluation (Table 5). The menisci were described in all the examined cases as moderately echogenic structures. Their external portion have been appreciated as clearly visible structures in most cases. (*ex vivo* in MM 69.23% LM 61.53%; *in vivo* in MM 70%, LM 50%), with the internal one mostly heterogeneous (in *ex vivo* MM 76.92% LM 69.23%, *in vivo* MM 70%, LM 80%). In the corpses, the shape of the medial meniscus was clearly triangular in 10 knees (76.92% of cases), while the lateral meniscus was clearly triangular in 53.85% of cases.

Table 5. *Ex vivo* results of ultrasound evaluation of the menisci

Criteria	Ultrasound examination	Medial Meniscus	Lateral Meniscus
Overall visibility of the external portion of the meniscal body	Not visible	0	0
	Barely visible	2	2
	Moderately visible	2	3
	Clearly visible	9	8
Appearance of the internal structure	Non Homogeneous	10	9
	Homogeneous	3	4
Shape	Not triangular	1	2
	Partially triangular	2	4
	Clearly triangular	10	7



Figure 3. Lateral longitudinal scan of the lateral meniscus

*In vivo*, the shape of the medial meniscus was clearly triangular in 60% of cases (6 knees), while the lateral meniscus was so in 40% of cases. The medial meniscus showed overall visibility, both *ex vivo* and *in vivo*, slightly higher than that of the lateral meniscus;

moreover, the typical triangular meniscal aspect was also more easily assessed in the medial meniscus. These observations are in agreement with what Van der Vekens et al. (2019) described. The superior ultrasound visibility of the medial meniscus compared to the lateral one represents a significant diagnostic advantage, as the medial meniscus represents the most commonly affected structure by CrCL rupture (Rey et al., 2014; Ritzo et al., 2014). Unlike what has been published by various authors (Kramer et al. 1999; Mahn et al., 2005; Soler et al. 2007), who attributed to the menisci a homogeneous aspect, in our paper, in line with Van der Vekens et al. (2019), menisci often presented a typical heterogeneous aspect. The hypochoic focal areas we considered to be the ultrasound representation of the radial meniscal fibers transversely from the ultrasound beam (Kambic & McDevitt, 2005; Van der Vekens et al., 2019). The patellar tendon, in agreement with Soler and colleagues (2007) was visible in all cases both *ex vivo* and *in vivo*, presenting a hyperechoic aspect in all cases comparing to the infrapatellar fat pad, with a clear hyperechoic and a fibrillar pattern and a linear and clearly visible contour.

In the *in vivo* study an innovative ultrasound approach to the knee was proposed: the caudal femoral-tibial scan. The idea of using this method was born with the aim of investigate the menisci as fully as possible, in fact the Lateral sagittal scan allows us to evaluate only a limited portion. By positioning the probe oriented transversely on the caudal surface of the knee, it was possible to appreciate, in all the joints taken into consideration, the profile of the femoral condyles. Moreover, by orienting the probe longitudinally it was possible to visualise in all the joints a small caudal portion of the menisci. Caudal scans were carried out with a convex or linear probe according to the animal examined. In the Labrador, in Dobermann, in Pitbull and in a large mixed breed, was used a low frequency convex probe. In the Weimaraner and in the medium-sized mixed breed was used the linear probe. In all knees scanned (12/12, 100%) the medial meniscus and the lateral meniscus were correctly identified by longitudinal scan. Furthermore, in all the dogs (12/12, 100%) the profile of the femoral condyles was correctly

highlighted in the transverse scan. Through this method, the caudal portion of the meniscal body was visible, allowing to evaluate a part of the menisci usually not distinguished by ultrasound. The caudal scan therefore, expanding the portion of the meniscus visible ultrasonographically, could facilitate the diagnosis of secondary meniscal lesions, which commonly occur in the caudal portion of the medial meniscus (Pozzi et al., 2006). This new ultrasound approach, allowing to evaluate also the profile of the femoral condyles, could be used, in the future, as an aid in the diagnosis of osteochondritis dissecans (OCD) in the knee. It is now known that similar pathologies affecting the cartilage profile, such as the OCD of the caudal humeral head, can often also be diagnosed by ultrasound (Cook, 2016).

According to our knowledge, this is the first study in Veterinary Medicine that described accurately the differences between the visualization of knees CT scans based on the different algorithm chosen (Tables 6 and 7).



Figure 4. Tomographic aspect of the CrCL (arrow) in para-sagittal scan with hard tissue algorithm

For this reason, after evaluating the CT images both with an algorithm for hard tissues and one for soft tissues we described the imaging differences of the two settings. In previous studies (Samii & Dyce, 2004; Soler et al., 2007) the lateral meniscus-femoral ligament (LMFL) was only identified and never thoroughly described. In our work the LMFL was described using the same evaluation scales used for cruciate ligaments. By applying an

algorithm for hard tissues, the bone was represented with a high image detail, making the demarcation between medullary and cortical. Quite the opposite, using a soft tissue algorithm the bone was represented in all cases exuberant and indefinite. Using a soft tissue algorithm cruciate ligaments, meniscus-femoral ligaments and menisci showed a radio-density similar to each other but higher than the infrapatellar fat pad. These observations agree with what previously described (Soler et al., 2007). By applying a hard tissue window, the intra-articular ligament structures were less visible than those assessed by using the soft tissue algorithm. The ligaments described by the hard tissue algorithm also exhibited a lower visibility of the ligamentous contour than those described with the soft tissue setting. Furthermore, the LMFL resulted, both using the algorithm for hard tissue than soft tissue, less visible than the cranial and caudal cruciate ligaments. However, in neither case the ligamentous structures appeared clearly visible and well contoured overall. Using a hard tissue algorithm, the internal structure of the ligaments always appeared homogeneous, while using a soft tissue setting in some cases the internal ligament structure appeared heterogeneous. It is important to underline that the ligamentous structures with neither of the two algorithms presented an anatomical detail such as to be able to investigate any injuries. The menisci were better visible through the application of a soft tissue algorithm. Despite the soft tissue algorithm providing superior meniscal detail, through both algorithms the menisci were less visible than the ligaments, underlining the obvious limitations of the method in investigating these structures. The

menisci, as well as the ligaments, also presented a more inhomogeneous appearance when examined using the soft tissue algorithm. In our opinion, the visualization of an inhomogeneous radio-density pattern is related to the superior anatomical detail architecture obtained with the soft tissue algorithm. In CT scans following the inoculation of the contrast medium, the ligamentous structures showed an overall visibility higher than the one described in the pre-arthrographic scans. The contrast medium showed a variable distribution based on the intra-articular structure taken under examination: the CrCL and the CaCL were well contoured by the contrast medium being always visible, in most cases having a good or moderate visibility. The LMFL has been surrounded less by the contrast medium, being not visible in 2 anatomical preparations. The worst distribution of the contrast medium occurred at the meniscal level; despite this, the menisci were found however visible in all anatomical preparations, showing higher overall visibility than the pre-arthrographic scan. Despite the fact that the volume and concentration of inoculated iodinated contrast medium concurred with what is described in the bibliography (Gielen & Van Bree, 2018), the fluid distribution was not uniform throughout the joint cavity. This phenomenon is partly associated with the onset of post-mortem alterations. In addition, it is possible that the more caudal structures do not receive the same amount of contrast as the cranial ones. The poor arthrographic delineation of the menisci is instead in agreement with what described by Samii et al. (2009), according to which CTA is a diagnostic method that presented gaps in the identification of meniscal tears.

Table 6. *Ex vivo* results of the tomographic evaluation with Hard tissue algorithm scans of Cranial (CrCL) and Caudal (CaCL) cruciate ligament, lateral meniscus-femoral ligament (LMFL), medial (MM) and lateral meniscus (LM)

<b>Criteria</b>	<b>TC-HAlgo</b>	<b>CrCL</b>	<b>CaCL</b>	<b>LMFL</b>	<b>MM</b>	<b>LM</b>
<i>Overall visibility</i>	Not visible	3	3	5	3	2
	Barely visible	5	5	3	8	9
	Moderately visible	3	3	3	0	0
	Clearly visible	0	0	0	0	0
<i>Visibility of the contour</i>	Not visible	3	3	5	3	2
	Barely visible	7	7	5	8	9
	Moderately visible	1	1	1	0	0
	Clearly visible	0	0	0	0	0
<i>Appearance of the internal structure</i>	Non Homogeneous	0	0	0	0	0
	Homogeneous	8	8	6	8	9

Table 7. *Ex vivo* results of the tomographic evaluation with Soft tissue algorithm scans of Cranial (CrCL) and Caudal (CaCL) cruciate ligament, lateral meniscus-femoral ligament (LMFL), medial (MM) and lateral meniscus (LM)

Criteria	TC-SAlgo	CrCL	CaCL	LMFL	MM	LM
Overall visibility	Not visible	2	1	1	2	2
	Barely visible	3	4	6	6	6
	Moderately visible	6	6	4	3	3
	Clearly visible	0	0	0	0	0
Visibility of the contour	Not visible	2	1	1	2	2
	Barely visible	4	6	7	7	7
	Moderately visible	5	4	3	2	2
	Clearly visible	0	0	0	0	0
Appearance of the internal structure	Non Homogeneous	1	2	2	4	4
	Homogeneous	8	8	6	5	5

Table 8. *Ex vivo* results of the computed tomography arthrography (CTA) evaluation of Cranial (CrCL) and Caudal (CaCL) cruciate ligament, lateral meniscus-femoral ligament (LMFL), medial (MM) and lateral meniscus (LM)

Criteria	CTA	CrCL	CaCL	LMFL	MM	LM
Overall visibility	Not visible	0	0	2	0	0
	Barely visible	3	3	2	7	5
	Moderately visible	5	5	4	4	6
	Clearly visible	3	3	3	0	0
Distribution of the contrast medium	Low	0	0	2	1	0
	Moderate	5	6	3	8	9
	Good	6	5	6	2	2
Appearance of the internal structure	Non Homogeneous	1	2	1	0	1
	Homogeneous	10	9	8	11	10

Still according to Samii et al. (2009), CTA represents a sensitive and specific method in the identification of CrCL injury. However, a clarification must be made: as described by Vande Berg et al. (2002) and Han et al. (2008), most of the partial ruptures of the CrCL are not acute but chronic; in addition, the knee affected by this pathological condition generally presents abundant effusion and fibrosis of variable degree that could alter the interpretation of the images. For this reason, the use of CTA in order to diagnose a partial rupture of the CrCL is a controversial procedure still under investigation. The internal structure of ligaments and menisci appreciated in CTA, unlike what was seen using a soft tissue algorithm was generally homogeneous. In our opinion, the high peripheral radio-density of the ligamentous structures and meniscal ligaments conferred by the medium contrast may have reduced the anatomical detail of the ligamentous and internal meniscal surface.

## CONCLUSIONS

The goal of this *ex vivo* study is to deepen the knowledge on the ultrasound anatomy of the

main intra-articular structures of the dog's knee, assessing the strengths and criticalities of the diagnostic method.

From the results obtained, ultrasonography is a valid diagnostic method in visualizing the cranial-distal part of the CrCL in dogs weighing more than 25 kg. Moreover, the ultrasound examination is capable of evaluating the internal meniscal structure with great anatomical detail. Given the scientific progress associated with the orthopedic diagnostic imaging, it is likely that in the next few years, particular interest will be focused on the ultrasonographic diagnosis of lesions affecting the CrCL and menisci.

## REFERENCES

- Banfield, C.M., Morrison, W.B. (2000). Magnetic Resonance arthrography of the canine stifle joint: technique and application in eleven military dogs. *Veterinary Radiology and Ultrasound*, 41 200-213.
- Buote N., Fusco J., Radasch R. (2009). Age, tibial plateau angle, sex, and weight as risk factors for contralateral rupture of the cranial cruciate ligament in Labradors. *Veterinary Surgery*, 38: 481-489.
- Cabrera S.Y., Owen T.J., Mueller M.G., Kass P.H. (2008). Comparison of tibial plateau angles in dogs with unilateral versus bilateral cranial cruciate ligament rupture: 150 cases (2000-2006). *Journal of*

- the American Animal Hospital Association*, 232:889-892.
- Cook C.R. Ultrasound imaging of the musculoskeletal system. (2016). *Veterinary Clinics of North America: Small Animal Practice*, 46:355-371.
- Cook J. (2010). Epidemiology of Cranial Cruciate Ligament Rupture. In: *Advances in the Canine Cranial Cruciate Ligament*. Muir P.(eds), Wiley-Blackwell; 3: 95-100.
- Cook J.L., Luther J.K., Beetem J., Karnes J., Cook C.R. (2010). Clinical comparison of a novel extracapsular stabilization procedure and Tibial Plateau Leveling osteotomy for treatment of cranial cruciate ligament deficiency in dogs. *Veterinary Surgery*, 39: 315-323.
- De Bruin T., De Rooster H., Bosmans T., Duchateau L., van Bree H., Gielen I. (2007). Radiographic assessment of the progression of osteoarthritis in the contralateral stifle joint of dogs with a ruptured cranial cruciate ligament. *Veterinary Record*, 161:745-750.
- Duval J.M., Budenberg S.C., Flo G.L., Sammarco J.L. (1999). Breed, sex, and body weight as risk factors for rupture of the cranial cruciate ligament in young dogs. *Journal of the American Veterinary Medical Association*, 215: 811-814.
- Elkins A.D., Pechman R., Kearney M.T., Herron M. (1991). A retrospective study evaluating the degree of degenerative joint disease in the stifle joint of dogs following surgical repair of anterior cruciate ligament rupture. *Journal of the American Animal Hospital Association*; 27:533-540.
- Fuller M.C., Hayashi K., Bruecker K.A., Holsworth I.G., Sutton J.S., Kass P.H., Kantrowitz B.J., Kapatkin A.S. (2014). Evaluation of the radiographic infrapatellar fat pad sign of the contralateral stifle joint as a risk factor for subsequent contralateral cranial cruciate ligament rupture in dogs with unilateral rupture: 96 cases (2006– 2007). *Journal of the American Animal Hospital Association*, 244; 328-338.
- Fuller M.C., Kapatkin A.S., Bruecker K.A., Holsworth I.G., Kass P.H., Hayashi K. (2014). Comparison of the tibial mechanical joint orientation angles in dogs with cranial cruciate ligament rupture. *Canadian Veterinary Journal*, 55: 757-764.
- Galloway R.H., Lester S.J. (1995). Histopathological evaluation of canine stifle joint synovial membrane collected at the time of repair of cranial cruciate ligament rupture. *Journal of the American Animal Hospital Association*, 31:289-294.
- Gambardella P.C., Wallace L.J., Cassidy F. (1981). Lateral suture technique for management of anterior cruciate ligament rupture in dogs: a retrospective study. *Journal of the American Animal Hospital Association*, 17: 33-38.
- Gielen I., van Bree H. (2018). Computed Tomography (CT) of the Stifle. In: *Advances in the Canine Cranial Cruciate Ligament*, Muir P.(eds), Wiley-Blackwell, 20:141-154.
- Grierson J., Asher L., Grainger K. (2011). An investigation into risk factors for bilateral canine cruciate ligament rupture. *Veterinary and Comparative Orthopaedics and Traumatology*, 24: 192-196.
- Griffon D.J. (2010). A review of the pathogenesis of canine cranial cruciate ligament disease as a basis for future preventive strategies. *Veterinary Surgery*, 39: 399-409.
- Han S., Cheon H., Cho H., Kim J., Kang J.H., Yang M.P., Lee Y., Lee H., Chang D. (2008). Evaluation of partial cranial cruciate ligament rupture with positive contrast computed tomographic arthrography in dogs. *Journal of Veterinary Science*, 4:395-400.
- Heffron L.E., Campbell J.R. (1978). Morphology, histology and functional anatomy of the canine cranial cruciate ligament. *Veterinary Record* 102: 280-283.
- Johnson J.A., Austin C., Breur G.J. (1994). Incidence of canine appendicular musculoskeletal disorders in 16 veterinary teaching hospitals from 1980 to 1989. *Veterinary and Comparative Orthopaedics and Traumatology*, 7: 56-59.
- Kambic H.E., McDevitt C.A. (2005). Spatial organization of types I and II collages in the canine meniscus. *Journal of Orthopedic Research*, 23:142–9.
- Kramer M., Stengel H., Gerwing M., Schimke E., Sheppard C. (1999). Sonography of the canine stifle. *Veterinary Radiology and Ultrasound*, 40:282-293.
- Mahn M.M., Cook J.L., Cook C.R., Balke M.T. (2005). Arthroscopic verification of ultrasonographic diagnosis of meniscal pathology in dogs. *Veterinary Surgery*, 34:318-323.
- Marino D.J., Loughin C.A. (2010). Diagnostic Imaging of the Canine Stifle: A Review. *Veterinary Surgery*, 3:284-95.
- Ohlerth S., Lang J., Scheidegger J., Nötzli H., Rytz U. (2001). Magnetic resonance imaging and arthroscopy of a discoid lateral meniscus in a dog. *Veterinary and Comparative Orthopedy and Traumatology*, 14:90-94.
- Plesman R., Gilbert P., Campbell J. (2013). Detection of meniscal tears by arthroscopy and arthrotomy in dogs with cranial cruciate ligament rupture: a retrospective, cohort study. *Veterinary and Comparative Orthopedy and Traumatology*, 26:42-46.
- Pozzi A., Hildreth B.E., Rajala-Schulz P.J. (2008). Comparison of arthroscopy and arthrotomy for diagnosis of medial meniscal pathology: an ex vivo study. *Veterinary Surgery*, 37:749-755.
- Pozzi A., Kowaleski M.P., Apelt D., Meadows C., Andrews C.M., Johnson K.A. (2006). Effect of medial meniscal release on tibial translation after tibial plateau leveling osteotomy. *Veterinary Surgery*, 35:486-494.
- Rey J., Fischer M.S., Böttcher P. (2014). Sagittal joint instability in the cranial cruciate ligament insufficient canine stifle. Caudal slippage of the femur and not cranial tibial subluxation. *Tierärztliche Praxis Ausgabe K: Kleintiere - Heimtiere*, 42:151-156.
- Ritzo M.E., Ritzo B.A., Siddens A.D., Summerlott S., Cook J.L. (2014). Incidence and type of meniscal injury and associated long-term clinical outcomes in

- dogs treated surgically for cranial cruciate ligament disease. *Veterinary Surgery*, 43: 952-958.
- Ritzo M.E., Ritzo B.A., Siddens A.D., Summerlott S., Cook J.L. (2014). Incidence and type of meniscal injury and associated long-term clinical outcomes in dogs treated surgically for cranial cruciate ligament disease. *Veterinary Surgery*, 43: 952- 958.
- Samii V.F., Dyce J. (2004). Computed Tomographic Arthrography of the normal canine stifle. *Veterinary Radiology and Ultrasound*, 45:402-406.
- Sanchez-Bustinduy M., de Medeiros M.A., Radke H., Langley-Hobbs S., McKinley T., Jeffery N. (2010). Comparison of kinematic variables in defining lameness caused by naturally occurring rupture of the cranial cruciate ligament in dogs. *Veterinary Surgery*, 39: 523-530.
- Scrivani P.V. (2018). Magnetic Resonance Imaging of the Stifle. In: *Advances in The Canine Cranial Cruciate Ligament*, Miur P. (eds), WILEY Blackwell, 155-163.
- Soler M., Murciano J., Latorre R., Belda E., Rodríguez M.J., Agut A. (2007). Ultrasonographic, computed tomographic and magnetic resonance imaging anatomy of the normal canine stifle joint. *Veterinary Journal*, 174: 351-361.
- Thieman K.M., Tomlinson J.L., Fox D.B., Cook C., Cook J.L. (2006). Effect of meniscal release on rate of subsequent meniscal tears and owner-assessed outcome in dogs with cruciate disease treated with tibial plateau leveling osteotomy. *Veterinary Surgery*, 35: 705-710.
- Van der Vekens E., de Bakker E., Bogaerts E., Broeckx B.J.G., Ducatelle R., Kromhout K., Saunders J.H. (2019). High-frequency ultrasound, computed tomography and computed tomography arthrography of the cranial cruciate ligament, menisci and cranial meniscotibial ligaments in 10 radiographically normal canine cadaver stifles. *BMC Veterinary Research*, 14:146.
- Vande Berg B.C., Lecouvet F.E., Poilvache P., Dubuc J.E., Maldague B., Malghem J. (2002). Anterior cruciate ligament tears and associated meniscal lesions: assessment at dual-detector spiral CT arthrography. *Radiology*, 223: 403-409.
- Vande Berg B.C., Lecouvet F.E., Poilvache P., Maldague B., Malghem J. (2002). Spiral CT arthrography of the knee: technique and value in the assessment of internal derangement of the knee. *European Radiology*, 12: 1800-1810.
- Witsberger T.H., Villamil J.A., Schultz L.G., Hahn A.W., Cook J.L. (2008). Prevalence of and risk factors for hip dysplasia and cranial cruciate ligament deficiency in dogs. *Journal of the American Animal Hospital Association*, 232: 1818-1824.